This is a peer-reviewed, accepted author manuscript of the following conference paper: Al-Moathin, A, Zhong, M, Al-Taai, Q, et al. 2023, Characterization of a compact wideband microwave metasurface lens for cryogenic applications. in 101st ARFTG Microwave Measurement Conference: Challenges in Complex Measurement Environments, IEEE, Piscataway, NJ. https://doi.org/10.1109/ARFTG57476.2023.10279542

Characterization of a Compact Wideband Microwave Metasurface Lens for Cryogenic Applications

Ali Al-Moathin[1], Mingyan Zhong[1], Qusay Al-Taai[1], Yunan Jiang[1], Michael Farage[1], Jalil ur Rehman Kazim[1], Muhammad Zulfiqar Ali[2], Fatemeh Nikbakhtnasrabadi[1], Megan Powell[3], Prince Khatri[3], Manoj Stanley[4], Alessandro Rossi[3,4], Hadi Heidari[1], Muhammad Ali Imran[1], Qammer H. Abbasi[1], Nick M. Ridler[4], Martin Weides[1], Chong Li[1]

[1]University of Glasgow, Glasgow, UK, [2]Oxford Instruments NanoScience, Oxon, UK, [3]University of Strathclyde, Glasgow, UK, [4]National Physical Laboratory, London, UK

***Abstract* — In this paper, we present characterization of a compact flat microwave lens operating between 6 GHz and 14 GHz using a near field scanning system. An X-band horn antenna and open-end rectangular waveguide were used as an illumination source and probe, respectively. |S21| is measured as the probe antenna moves on a plane orthogonal to the optical axis vertically and horizontally. The lens is made of a metasurface layer that is sandwiched by two layers of cross-oriented gratings. The overall dimension of the lens is 10 cm in diameter and 0.57 cm in thickness. The measurement results show that the lens's focal length is 8 cm, and the beamwidth (full width at half maximum (FWHM)) is 3.5 cm. A transmission efficiency of over 90% and a cross-polarization gain of 25 dB were achieved over the entire bandwidth. The measurement results at room temperature are in good agreement with numerical simulations. The proposed lens will be used in a cryogenic environment e.g. dilution refrigerators for quantum computing systems. More results at cryogenic temperature e.g. below 30 K will be shown at the conference.**

***Index Terms* — Lens, Metasurface, X-band, Broadband.**

I. Introduction

Microwave lenses (MWLs) are used to collimate, focus and redirect microwave beams for applications such as wireless communication, imaging, and instrumentation. At millimeter-wave and terahertz frequencies, where high attenuation in free space propagation is expected, microwave lenses are used to boost the signals [1,2]. Recently, we have secured a research grant, EPIQC [3], to investigate the replacement of bulky coaxial cables in quantum computing systems by wireless technology. MWLs will be implemented to guide the control/readout signals for superconductor qubits, usually 6 GHz - 10 GHz, between cryogenic stages and chambers. Due to the restricted space within the dilution refrigerator, a microwave lens operating between 6 GHz and 10 GHz must have a diameter smaller than 10 cm. Several types of MWLs have been developed in the past, such as metal zone plates [4], dielectric Fresnel lenses [5,6], or patch antennas [7,8]. However, they either cause feedback interference, positioning sensitivity, zone edge blockage, narrow operational bandwidth or have low efficiencies [5,9]. MWLs based on metamaterials such as gradient index lenses and Luneburg lenses have recently been demonstrated for their compactness, wide operational bandwidth, and high efficiency [10-12]. However due to complex fabrication process of such MWLs, metasurface based lenses constructed using standard photolithography manufacturing processes are a more attractive option [13]. Although three separate layers, i.e. polarizer, a metasurface lens, and cross-polarizer, are required, each layer can be easily fabricated using a standard PCB process and final assembly is also straightforward. A very high transmission efficiency, i.e., more than 90% across a wide bandwidth is achievable. However, the lens reported in [13] is far too large for this application. The lens was redesigned based on the same principle, achieving similar performance as [13], but with a diameter of 10 cm. In this summary, we present design, fabrication and room-temperature characterization results of the lens. We will reveal detailed cryogenic results at the conference.

II. Unit Cells and Lens Design

The proposed lens has three layers: cross-polarized polarizer (top), a metasurface lens (middle), and co-polarized polarizer (bottom). The working principle of the lens can be found in [13]. We briefly describe the design of the lens for completeness. The operational frequency of the metasurface-based MWL is governed by its unit cell having a sub-wavelength period. The period of the lens is determined by the lowest operating frequency and an upper frequency limit at which that period will result in the onset of grating lobes. To reduce both the operational frequency and lens size, a material with higher permittivity must be used. i.e., it allows constricting small unit cells for the same operational frequency or below. However, small unit cells become problematic, from the fabrication perspective, because their feature sizes are beyond the capability of conventional printed circuit board (PCB) technology. After careful consideration, Roger's TMM 10i that has a dielectric constant of 9.8 and loss tangent of 0.002 at 10 GHz was selected for this work.

Fig. 1 (a) shows a schematic of the square unit, where L is the arm length of the cell, w is the width of the metal wire, and d is the period of the square unit. The fundamental unit cell, i.e., central cell of the lens with relative phase shift of 0º, was first designed and optimized for the best performance in terms of lowest reflectance, wider operational bandwidth, and higher transmittance (over 90%). The phase shift, $\Delta\varphi(x,y)$, as a

function of radius, $r(x,y)$, for the final lens design has a nonlinear distribution and is governed by

$$\Delta\varphi(x,y) = \frac{2\pi}{\lambda}\left(\sqrt{f^2 + r(x,y)^2} - f\right) \quad (1)$$

where f is the designed focal length of the lens and λ is the operating wavelength.

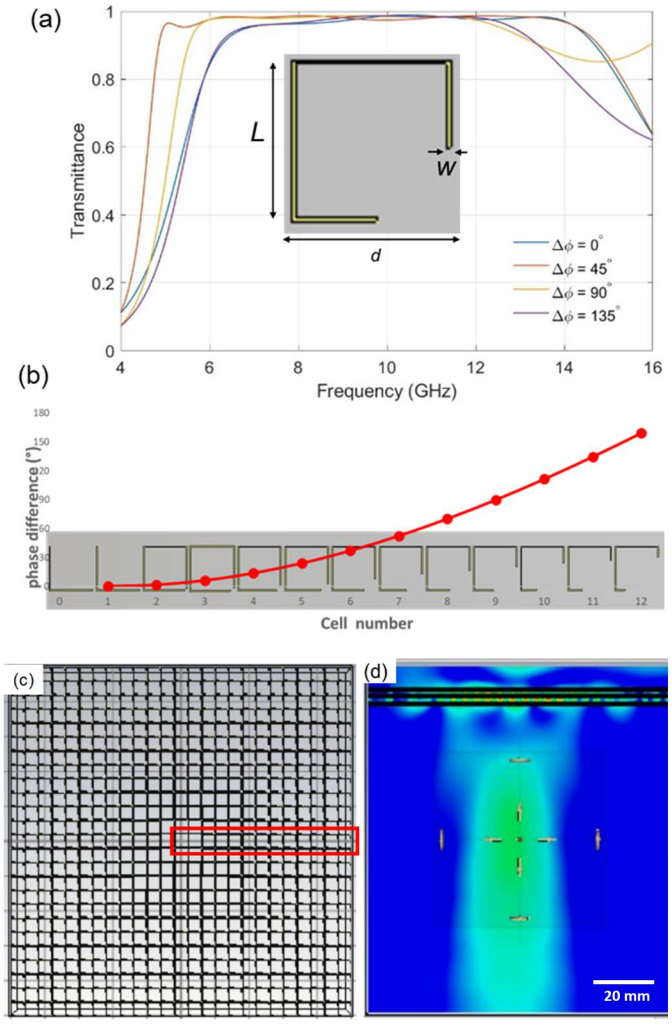

Fig.1. (a) Illustration of the unit cell and the simulated transmittance of unit cells providing phase shift of 0º, 45º, 90º, and 135º with transmission efficiency of over 90% over wide bandwidth (b) the unit cell arrangement for the final lens design. (c) the final lens and (d) the numerical simulation of the lens with plane wave incident from the top.

The constraint of overall size of the lens has put the limit on the number of unit cells and the total phase shift for the final lens. After several iterations of optimization, the final optimized phase shift was from 0º to 160º and the corresponding 12-unit cells from the center to the right edge is shown in Fig. 1 (b). Fig.1 (c) shows the top view of the metasurface layer and (d) shows the side view of the simulated lens that has a cross-polarized grating layer on the top and a co-polarized grating layer on the bottom. CST Studio was used for the simulations. In Fig. 1(d), a plane wave was illuminated onto the lens from the top and the lens focuses the beam on the other side.

The gratings consist of periodic metal strips and gaps. The width of the strip is 0.2 mm and the gap between strips is 0.6 mm.

III. Fabrication

As stated, material used for the three layers of the MWL was Roger's TMM10i, which was covered by copper on both sides. With standard PCB manufacturing processes, the smallest feature size is in tens of micrometers which is unfortunately not suitable for this work. We have explored several different fabrication processes, considering the survivability of Rogers TMM10i to the chemical solutions used in semiconductor photolithography. The final workable process using photolithography is as follows: the material was first dipped into a wet solution consisting of copper sulphate pentahydrate ($CuSO_4$), Hydrochloric (HCl) acid, and H_2O with a concentration of 0.3:1:1 respectively to remove the copper claddings on both sides. The clean surface was then spun with S1818 photoresist at a speed of 3000 rpm which gives roughly 2 µm of photoresist height. The coated surface was then exposed to a MA6 aligner with a chrome photomask where the lens or grating pattern was formed. After the exposure, the sample was developed in microposit:H_2O solution (1:1 by volume) for 30 minutes and then cleaned with O_2 plasma to remove any remaining resist at the exposed areas. Next, the required metasurface structure was formed by depositing Al followed by Ag with thicknesses of 20 nm and 400 nm, respectively, using Plassys PECVD, the sample was then dipped in Acetone at 50 °C for 2 hours to lift-off the remaining resist and cleaned. Fig.2 show the final fabricated gratings and metasurfaces. The lens was finally assembled with two gratings oriented in 90º and in-between is the metasurfaces. The three layers were separated evenly by 5 mm.

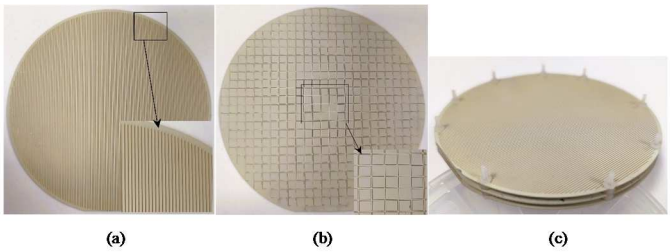

Fig. 2. Photos of the fabricated (a) gratings, (b) metasurfaces and (c) assembled three-layer lens consisting of a metasurface layer sandwiched by two cross-polarized gratings.

IV. Measurement Setup and Results

Figure 3 (a) shows the measurement setup used for testing the MWL. A standard gain horn and an open-ended waveguide both operating at X-band (8.2 GHz - 12.4 GHz) were used as a

source and a probe detector, respectively. The source antenna was fixed on a post and the probe antenna was mounted on a motorized two-dimensional linear scanning system that has two high-precision translation stages (+/- 5 µm accuracy) for vertical and horizontal scanning. The MWL was placed at the far-field zone from the source antenna, which is approximately 40 cm, to approximate plane-wave incidence to the MWL The fixture holding the MWL is made of extremely low loss, transparent material having a dialectic constant of 1.03. Microwave absorbers were attached to the probe antenna to avoid reflection from the stages. A Keysight E8361A vector network analyzer (VNA) was calibrated to the end of the coaxial cables, which were connected to the feeds of the horn and waveguide antennas, using a SOLT method with Keysight's 85052D calibration kits for the frequency range between 10 MHz and 18 GHz despite the cut-off frequencies of the antennas. A LabVIEW programme was developed to control the translation stages and the VNA [14].

We first scanned the horn antenna with lens support fixture but without the presence of the lens. Fig.3 (b) shows $|S_{21}|$ in dB at 8 GHz for cross-polarization between the horn antenna and the probe over a scanning area of 28 steps (the step size is 5 mm). Fig.3 (c) shows $|S_{21}|$ in dB at 8 GHz when the assembled lens was placed at 8 cm in front of the scanning plane. A clear focusing spot is visible and if comparing with Fig. 3(b), one can see a maximum of 25 dB gain is achieved in the center of the spot. Fig.3 (d) shows a cut along the center of vertical axis and it is normalized to the maximum value. The two notches at the sides of the central peak indicate the edge of the lens and the full width half power (- 3 dB) is approximately 3.5 cm. The results are in good agreement with numerical simulations.

To evaluate the lens performance at cryogenic temperatures, we employed a cryogenic calibration technique to determine the calibrated S-parameters of the antenna-lens-antenna system at 4 K, using an in-situ microwave calibration unit [15]. The obtained frequency-domain S-parameter data was then transformed to the time domain using the inverse Fourier transform, and time-domain gating was applied to eliminate the antenna response. This approach allowed us to estimate losses in the lens and comprehend its reflection performance from the lens interfaces.

It is important to note that the overall loss of the lens is a result of the dielectric loss in the substrate material and the ohmic loss due to the finite conductivity (non-zero resistivity) of the conductor material. Since we used gold, which has high conductivity, to construct the transmission lines and microwave circuits at cryogenic temperatures, the ohmic loss is negligible. Consequently, heating is primarily caused by the losses in the dielectric substrate material. The substrate material used in this study (TMM10i) has been demonstrated to exhibit very low loss tangent at cryogenic temperatures down to 4 K and is routinely employed as a substrate material for cryogenic applications [16].

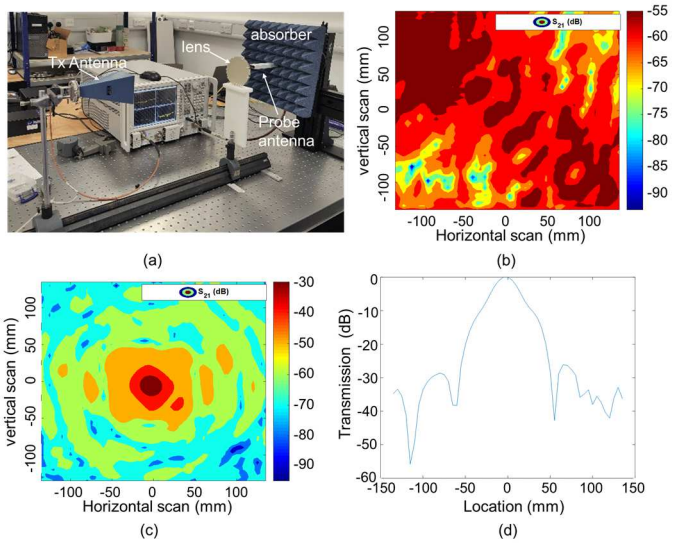

Fig. 3. (a) Illustration of the measurement setup with the lens under test. A standard gain horn antenna was placed on a post on the left and an open-end waveguide probe antenna was mounted on a 2D scanner on the right. (b) 2D plot of $|S_{21}|$ for cross-polarization scanning at 8 GHz i.e. polarization of the horn and the probe is orthogonal (c) 2D plot of $|S_{21}|$ with the lens at 8 cm in front of the probe antenna. (d) the cut along the center of the vertical scanning.

V. Conclusion

A near field 2D antenna scanner system with a VNA was implemented to characterize a compact metasurface-based microwave lens operating between 6 GHz and 14 GHz. Both numerical simulations and measurements demonstrate that the lens has a focal length of 8 cm and a beamwidth of 3.5 cm. We achieved a transmission efficiency of over 90% and a cross-polarization gain of 25 dB over the entire bandwidth. This lens is intended for use in a cryogenic environment, such as dilution refrigerators, for wireless quantum computing systems. The measurement results for the focal length, beamwidth, and transmission efficiency agree well with the numerical simulation results.

Acknowledgement

This work was supported by the Engineering and Physical Research Council, UK (Grant No. EP/W032627/1). The authors would like to thank the staff of the James Watt Nanofabrication Centre and Electronic Systems Design Centre at the University of Glasgow for their help and support. Special thanks are given to Mr. Zimo Zhao for developing the LabVIEW codes.

References

[1]. M. Abbasi et al., "Single-chip 220-GHz active heterodyne receiver and transmitter MMICs with on-chip integrated antenna," IEEE Trans. Microw. Theory Tech., vol. 59, no. 2, pp. 466-478, Feb. 2011, doi: 10.1109/TMTT.2010.2095028.

[2]. C. Li, J. Grant, J. Wang, and D. R. S. Cumming, “A Nipkow disk integrated with Fresnel lenses for terahertz single pixel imaging,” Opt. Express, vol. 21, 24452-24459, 2013.
[3]. https://gow.epsrc.ukri.org/ngboviewgrant.aspx?grantref=ep/w032627/1.
[4]. W. E. Kock, “Metal-lens antennas,” Proc. IRE, vol. 34, no. 11, pp. 828–836, 1946.
[5]. H. D. Hristov and M. H. A. J. Herben, “Millimeter-wave Fresnel-zone plate lens and antenna,” IEEE Trans. Microw. Theory Tech., vol. 43, no. 12, pp. 2779–2785, 1995.
[6]. T. A. Hill, J. R. Kelly, M. Khalily, and T. W. C. Brown, “Cascaded Fresnel lens antenna for scan loss mitigation in millimeter-wave access points,” IEEE Trans. Antennas Propag., vol. 68, no. 10, pp. 6879–6892, 2020.
[7]. D. T. McGrath, P. M. Proudfoot, and M. A. Mehalic, “The microstrip constrained lens,” Microw. J., vol. 38, no. 1, p. 24, 1995.
[8]. D. McGrath, “Planar three-dimensional constrained lenses,” IEEE Trans. Antennas Propag., vol. 34, no. 1, pp. 46–50, 1986.
[9]. W. Rotman, “Analysis of an EHF aplanatic zoned dielectric lens antenna,” IEEE Trans. Antennas Propag., vol. 32, no. 6, pp. 611–617, 1984.
[10]. Q. Ma, et al. “Broadband metamaterial lens antennas with special properties by controlling both refractive-index distribution and feed directivity.” Journal of Optics, vol. 20, no. 4, 045101, 2018.
[11]. R. Yang, W. Tang, Y. Hao and I. Youngs, "A coordinate transformation-based broadband flat Lens via microstrip array," IEEE Antennas Wirel. Propag. Lett., vol. 10, pp. 99-102, 2011, doi: 10.1109/LAWP.2011.2112328.
[12]. H. Ma, and T. Cui, “Three-dimensional broadband ground-plane cloak made of metamaterials.” Nat. Commun. vol. 1, no. 21, 2010. https://doi.org/10.1038/ncomms1023
[13]. A. K. Azad, A. V Efimov, S. Ghosh, J. Singleton, A. J. Taylor, and H.-T. Chen, “Ultra-thin metasurface microwave flat lens for broadband applications,” Appl. Phys. Lett., vol. 110, no. 22, p. 224101, 2017.
[14]. M. Farage, Z. Zhao, Q. Abbasi, and C. Li, “Evaluation of a 300 GHz near field antenna measurement system.” IET Colloquium on Millimetre-wave and Terahertz Engineering and Technology 2021, 17-18 Mar 2021.
[15]. L. Ranzani, et.al, “Two-port microwave calibration at millikelvin temperatures,” Rev. Sci. Instrum. vol. 84, 034704, Mar 2013.
[16]. Pascale Diener, F. Couëdo, C. Marrache-Kikuchi, M. Aprili, and J. Gabelli, “Cryogenic calibration setup for broadband complex impedance measurements,” AIP Conference Proceedings, 2014, 1610, ff10.1063/1.4893520